EFDA–JET–CP(12)04/17

S. Saarelma, M.N.A. Beurskens, D. Dickinson, A. Kirk, M. Leyland, C.M. Roach,
R. Scannell and H.R. Wilson and JET EFDA contributors

Pedestal Modelling Based on Ideal MHD and Gyrokinetic Stability Analyses on MAST and JET Plasmas

Pedestal Modelling Based on Ideal MHD and Gyrokinetic Stability Analyses on MAST and JET Plasmas

S. Saarelma[1], M.N.A. Beurskens[1], D. Dickinson[1,2], A. Kirk[1], M. Leyland[2], C.M. Roach[1], R. Scannell[1] and H.R. Wilson[2] and JET EFDA contributors*

JET-EFDA, Culham Science Centre, OX14 3DB, Abingdon, UK

[1]EURATOM-CCFE Fusion Association, Culham Science Centre, OX14 3DB, Abingdon, OXON, UK
[2]York Plasma Institute, Department of Physics, University of York, York, YO10 5DD, UK
** See annex of F. Romanelli et al, "Overview of JET Results",*
(23rd IAEA Fusion Energy Conference, Daejon, Republic of Korea (2010)).

Preprint of Paper to be submitted for publication in Proceedings of the
39th European Physical Society Conference on Plasma Physics, Stockholm, Sweden
2nd July 2012 - 6th July 2012

INTRODUCTION

The H-mode pressure pedestal is crucial for the confinement of a tokamak fusion device. In order to predict the height of the pedestal, we need to understand the instabilities controlling the pedestal evolution. Pedestal performance has been successfully predicted for several current tokamaks using the EPED model [1] which combines pedestal pressure gradient limiting Kinetic Ballooning Modes (KBM) with pedestal top pressure limiting peeling-ballooning modes to produce a prediction for the pedestal width and height.

In this paper, we exploit high resolution diagnosis of pedestal profiles from Type I ELM cycles on MAST and JET to perform MHD and gyrokinetic stability analyses that allow us to test rigorously the ideas behind the EPED model.

1. MAST PLASMAS

The width of the MAST edge pedestal increases during the ELM cycle, but the maximum pressure gradient stays almost constant after the rapid recovery immediately following the crash. By varying the fuelling during the discharge it is possible to vary Te,ped and thus collisionality. In high collisionality ($\nu_{*,\,ped} = 1.4$) pedestals only the density pedestal height increases during the ELMcycle, while in low collisionality ($\nu_{*,\,ped} = 0.6$) pedestals both the density and temperature increase (Fig.1). The n_e and T_e profiles were measured using Thomson scattering system with 130 radial points with 10mm radial resolution and fitted with a modified hyperbolic tangent function or *mtanh* (for details see [2] and references therein).

We use these profiles (and assume $T_i = T_e$) to reconstruct the equilibrium using the HELENA code[3]. The bootstrap current (j_{bs}) dominates the current profile in the edge region, and is calculated self-consistently using formulas in [4]. The low ν_* plasma has more bootstrap current, and, consequently lowermagnetic shear near the edge region. The flux surface averaged toroidal current density and q-profiles are plotted in Fig.2.

Both high and low collisionality plasmas start the ELM cycle by being stable to finite *n* ideal MHD modes (*n* is the toroidal mode number), but become unstable to these modes by the end of the ELM cycle. This is consistent with these modes producing the ELM trigger. The stability to the $n = \infty$ ideal ballooning modes differs in these two pedestals. In the high ν_* plasma with high magnetic shear, the pedestal is unstable to $n = \infty$ ballooning modes through the ELM cycle. The width of the unstable region follows the increasing width of the density pedestal [2]. On the other hand, the low ν_* plasma has low shear in the steep pressure gradient region and this gives access to second stability. Except for a narrow (<1% of poloidal flux) band near the very edge, the low ν_* pedestal is stable to $n = \infty$ ballooning modes. In a linear gyrokinetic analysis using GS2 [5], we find good correspondence between the KBM and $n = \infty$ idealMHD ballooningmode stability. Also by artificially reducing the bootstrap current in the equilibrium reconstruction it is possible to make the low ν_* pedestal unstable against the $n = \infty$ ballooning modes and KBMs.

In both cases we find unstable micro-tearing (MTM) modes in the pressure plateau at the top

of the pedestal. These modes are stabilised by increasing the density gradient. An artificial scan of pressure gradient (by increasing both density and temperature gradients consistent with the profile evolution observed in the experiment, but not increasing j_{bs} and adjusting q-profile self-consistently) at the "knee" of the pedestal ($\psi = 0.94$) midway through the ELM cycle demonstrates the stabilisation of MTMs ($0.5 < k_\theta \rho_i < 4$, k_θ is the poloidal wave number) and destabilisation of KBMs ($k_\theta \rho_i < 0.5$) as was found for high ν_* in [6]. The growth rate spectrum of this scan is shown in Fig.3. The widening of the steep pressure gradient region can be explained by this stability behaviour at the pedestal "knee". The steepening pressure profile reduces the MTM drive for turbulence reducing the transport until the KBM stability limit is reached, which stops the increase of ∇p.

2. JET PLASMAS

The JET pedestal profiles with varying degree of fuelling are measured using Thomson scattering system with 1cm radial resolution and fitted with mtanh-function. Pedestal evolution in high triangularity JET plasmas is different from MAST. We look at two shots at $\delta = 0.42$, $I_p = 2.5$MA, $B_t = 2.7$T with varying fuelling. In a high fuelling case (Pulse No: 79503, $G = 2.7\times10^{22}$el/s), the pedestal width does not markedly change after the initial recovery from the ELM. The pressure pedestal height increases in the early part of the ELM cycle, but then it saturates. The plasma sits close to the peeling-ballooning stability boundary most of the ELM cycle. In a low fuelling case (Pulse No: 79498, $G = 0.5\times10^{22}$ el/s) the pedestal density and temperature profiles get narrower and steeper during the ELM cycle only crossing the peeling-ballooning boundary at the end of the ELM cycle. In both cases the most unstable n at the crossing of the stability boundary is about 15. Full stability diagrams are shown in [7].

Due to high bootstrap current driven by the pressure gradient most of the JET pedestal is in the 2nd stable region $n = \infty$ throughout the ELM cycle. A narrow region between the pressure gradient peak and the plasma edge is marginally unstable. Similar to MAST, GS2 finds good correspondence between the ideal MHD $n = \infty$ ballooning mode and gyrokinetic KBM stability, i.e. most of the pedestal is stable to KBMs. As for MAST low ν_* pedestal removing the bootstrap current (removing the 2nd stability access) makes the entire pedestal unstable to KBMs Gyrokinetic analysis reveals that the JET pedestal top is dominated by Ion Temperature Gradient (ITG) modes, but we also find subdominant MTMs that are stabilised by the steepening of density gradient the same way as in MAST. However, the dominant ITG modes are not affected by the steepening of the density gradient.

CONCLUSIONS

Finite *n* stability analysis for the equilibria reconstructed during the different phases of the ELM cycle shows that both JET and MAST plasmas reach the Peeling-Ballooning (PB) limit before an ELM crash. The absence of KBMs shows that while the PB modes set the limit for the pedestal height, the pedestal recovery between ELMs in JET and MAST are controlled by different processes. ITER with high bootstrap current is likely to be KBMstable, like JET, making it difficult to predict

the pedestal based on KBM stability. On the other hand, the PB stability should be a robust limit for ITER pedestals. In all MAST and JET plasmas we find unstable MTMs at the pedestal top.

ACKNOWLEDGEMENTS

This work was funded by the RCUK Energy programme and EURATOM. The work was was carried out within the framework of EFDA.

REFERENCES

[1]. Snyder P.B., et al. Physics of Plasmas **16** (2009) 056118.

[2]. Dickinson D. et al., Plasma Phys. Controlled Fusion **53** (2011) 115010,

[3]. Huysmans G.T.A. et al., Proc. of Int. Conference Computational Physics, Amsterdam (1991) 371.

[4]. Sauter O., Angioni C., Lin-Liu Y.R., Physics of Plasmas, **6** (1999) 2834.

[5]. Kotschenreuther M., et al., Computational Physics Communication **88** (1995) 128

[6]. Dickinson D. et al., Physical Review Letters **108** (2012) 135002

[7]. Leyland M.J. et al. in preparation for submission to Nuclear Fusion

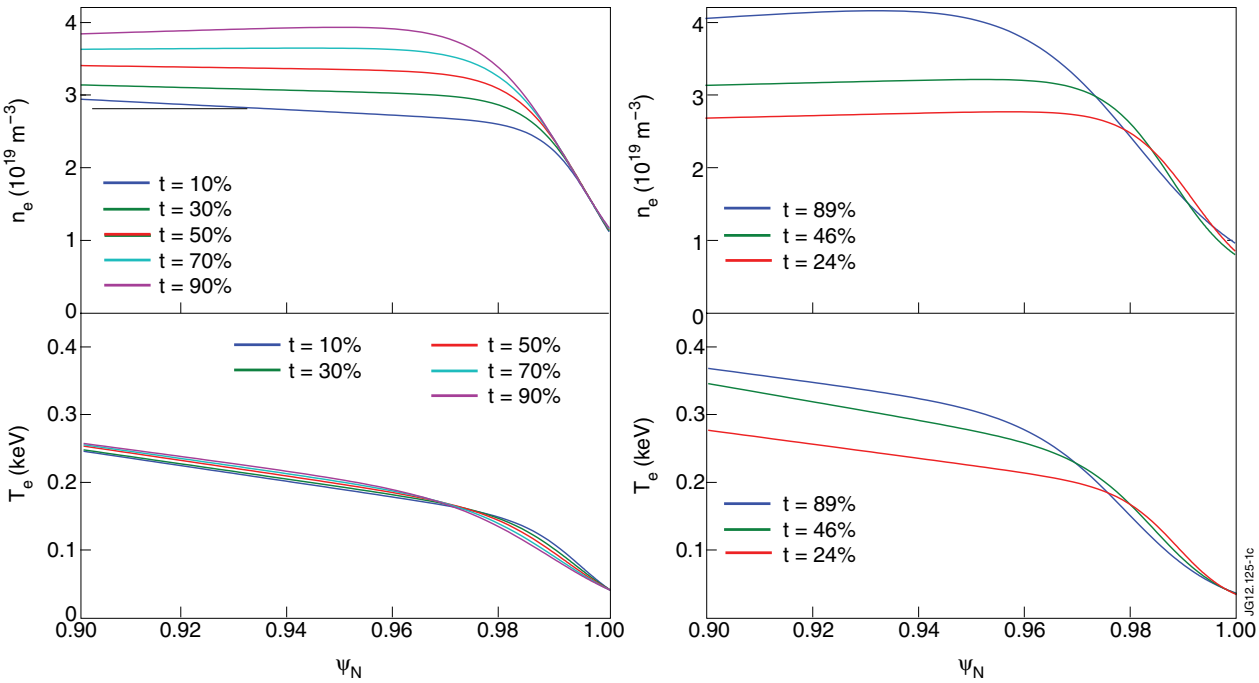

Figure 1: The n_e (top) and T_e (bottom) profile evolution during the ELM cycle in high (left) and low (right) collisionality MAST discharges. The labels represent the normalised time in the ELM cycle.

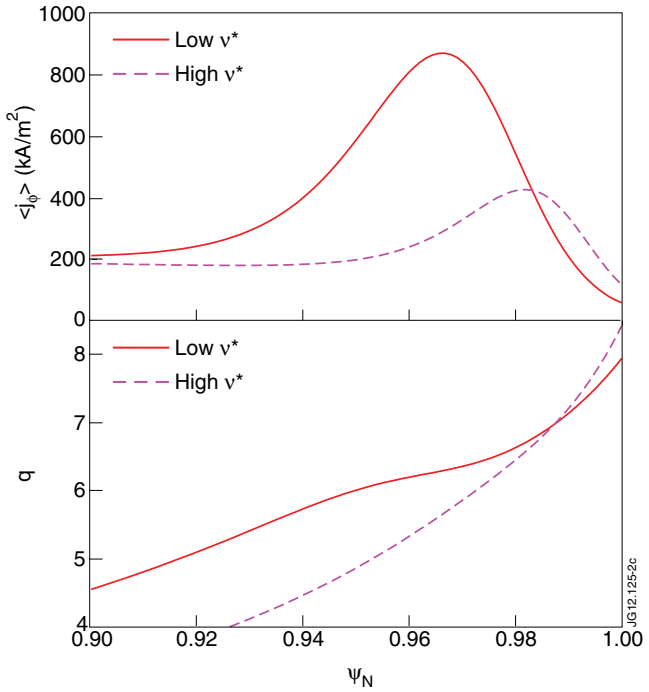

Figure 2: The toroidal current density and q-profile at the end of the ELM cycle in high and low ν_* MAST discharges.

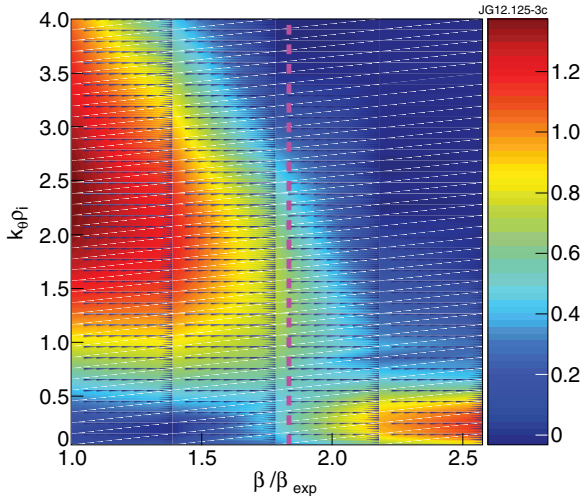

Figure 3: The growth rate spectrum at $\psi = 0.94$ at 46% of the normalised ELM cycle of the low ν_* MAST plasma when β' is varied from the experimental value. The vertical dashed line represents the pressure gradient values 8ms later in the ELM cycle.

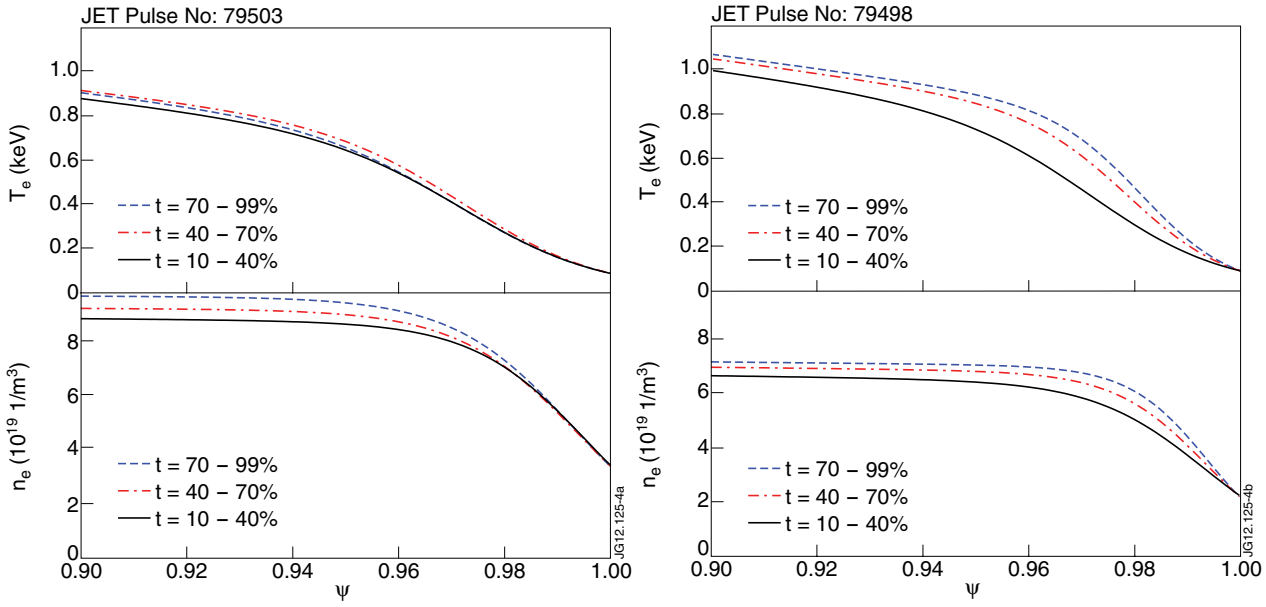

Figure 4: The density and temperature profile evolution during the ELM cycle in high (#79503) and low (#79498) fuelling JET discharges. The labels represent the normalised time in the ELM cycle.

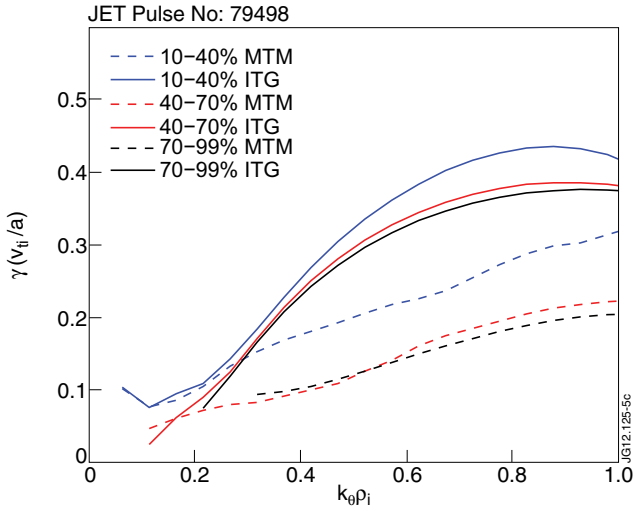

Figure 5: The growth rate spectrum of JET Pulse No: 79498 at the "knee" of the pedestal (ψ = 0.96) during the ELMcycle. The solid lines show the ITG modes and the dashed lines the MTMs.